



On-demand generation of singlet oxygen from a smart graphene-complex for the photodynamic treatment of cancer cells

Journal:	<i>Biomaterials Science</i>
Manuscript ID:	BM-ART-04-2014-000143.R1
Article Type:	Paper
Date Submitted by the Author:	21-May-2014
Complete List of Authors:	<p>Gu, Zhanjun; Institute of high energy physics, YAN, Liang; Chinese Academy of Sciences, Chang, Ya-Nan; Institute of High Energy Physics, Chinese Academy of Sciences, Yin, Wenyan; Institute of high energy physics, Key Laboratory for Biomedical Effects of Nanomaterials and Nanosafety Tian, Gan; Sichuan University, College of Chemistry Zhou, Liangjun; University of Chinese Academy of Sciences, College of Materials Science and Opto-Electronic Technology; Chinese Academy of Sciences, Institute of High Energy Physics Liu, Xiaodong; Chinese Academy of Sciences, Institute of High Energy Physics Xing, Gengmei; Institute of High Energy Physics, Zhao, Lina; Institute of High Energy Physics, CAS, Zhao, Yuliang; Institute of High Energy Physics, Chinese Academy of Sciences, CAS Key Lab for Biomedical Effects of Nanomaterials and Nanosafety, CAS Key Laboratory of Nuclear Analytical Techniques</p>

On-demand generation of singlet oxygen from a smart graphene-complex for the photodynamic treatment of cancer cells

Liang Yan,¹ Ya-Nan Chang,¹ Wenyan Yin,¹ Gan Tian,¹ Liangjun Zhou,¹ Xiaodong Liu,¹ Gengmei Xing,¹ Lina Zhao,¹ Zhanjun Gu^{*1} and Yuliang Zhao^{*1,2}

¹CAS Key Laboratory for Biomedical Effects of Nanomaterials and Nanosafety, Institute of High Energy Physics, Chinese Academy of Sciences (CAS), Beijing 100049, China

²National Center for Nanosciences and Technology of China, Beijing 100190, China

*Corresponding author: zjgu@ihep.ac.cn; zhaoyuliang@ihep.ac.cn

Abstract: Graphene oxide (GO) has been proved to be a highly efficient long-range quencher for various fluorescence processes which intrinsically work through photophysical mechanism similar with that of singlet oxygen generation (SOG). Under our hypothesis that GO may be capable of quenching SOG process, we hence design and synthesize a novel nanocomplex consisting of GO, photosensitizer and aptamer. We demonstrate that GO is an ideal platform functioning as the SOG controller which can reversibly quench and recover SOG depending on the interaction intensity between GO and photosensitizer, while simultaneously acting as a carrier for efficient loading and delivery of photosensitizers to cancer cells. Thus, during the delivery process, SOG of the nanocomplex can be completely inhibited by the quenching capacity of GO even though there is light; however, when nanocomplex enters into cancer cells where target molecules present, SOG is triggered by the target binding event and singlet oxygen is reversibly released from the nanocomplex, ultimately inducing significant cell death in the presence of light. This proof-of-concept study provides a new chemical strategy for creating low-toxic and highly-selective photodynamic therapy using hydrophilic GO-based systems.

Keywords: Graphene oxide; Aptamer; Photodynamic treatment; Single oxygen generation; Cancer cells

1. Introduction

Photodynamic therapy (PDT) has been emerging as a non-invasive therapeutic modality that uses photosensitizers (PSs), light and molecular oxygen for the local treatment of various diseases including cancer.¹⁻⁴ When illuminated by an appropriate light, the excited PSs transfer their energy to surrounding molecular oxygen, generating cytotoxic reactive oxygen species, such as singlet oxygen ($^1\text{O}_2$), that can effectively kill cancer cells *in situ*. Therefore, PDT offers many advantages over conventional therapeutics, such as high effectiveness, localized and specific tumor treatment and repetition of therapy without cumulative toxicity.^{5,6} However, there are still many drawbacks in the current PDT for clinical applications.^{7,8} In practice, many of the commonly used PSs possess hydrophobic nature and thus tend to aggregate in the physiological solution, rendering big challenges in delivery process and biocompatibility issues, and also causing the unwanted collateral damage to the normal tissues. In addition, the life time and diffusion range of $^1\text{O}_2$ from a photosensitizer (PS) used in the conventional PDT are very short, <200 ns and ~20 nm, respectively.^{9,10} Thus, it is essential to establish a chemical strategy for the hydrophilic PS system with a controllable singlet oxygen generation (SOG) to minimize the harm to the healthy cells/tissues, and enhance the PDT selectivity and efficacy.

To fully/partly meet the above requirement, nanomaterials such as gold, silica and carbon nanotube have been proposed as vehicles for the delivery of PDT agents.¹⁰⁻¹³ Among them, graphene oxide (GO) has implemented as a novel nanomaterial in the field of biomedicine. Owing to its unique 2-dimensional structure, abundant functional groups, large surface area, good biocompatibility and low-cost,^{14,15} GO has been widely explored as a novel vehicle for the delivery of drugs and biomolecules, such as siRNA and aptamers, to the target tissues.¹⁶⁻¹⁸ Taking together its ability of highly efficient tumor passive targeting,¹⁹ GO as a nanocarrier may enhance PS payload and improve tumor uptake over free PSs. Several groups have successfully employed GO as a delivery carrier of PSs, such as Chlorin e6 (Ce6) and hyaluronic acid, for killing tumor cells *in vitro* by light irradiation. Unfortunately, it is still difficult to optimally regulate SOG of PSs using GO-based delivery system. Thus, it is rather important to further develop a GO-based photoactivity switchable carrier for PDT, which may minimize the damage to healthy tissues.^{6,20-22} Recently, GO has been proved to be a highly

efficient long-range quencher for various fluorescence probes.²³ Considering that the photophysical mechanism of SOG should be similar to that of fluorescence process (Figure S1), we hence hypothesize that GO may be capable of quenching SOG. If this idea works, GO can function as a “cage” for controlling SOG by manipulating the distance between GO and PSs, and meanwhile use as the vehicle for efficient delivery of PSs to the diseased tissues, ultimately showing a controllable and enhanced PDT effects.

In this work, we first engineered a novel nanocomplex that combined a PS, an aptamer and GO for the controllable SOG (named GO/AP-PS). Figure 1 outlines how we incorporated the significant features of GO, aptamer and PS to form a simple yet rather efficient and elegant PDT agent. First, the aptamer was synthesized and then covalently attached to a PS (AP-PS). Second, by means of π -stacking interaction, the PS functionalized aptamer could tightly adsorb onto the GO surface. In the absence of a target molecule, PS would closely approximate the GO surface, causing both fluorescence and SOG were almost completely shut down. Significantly, the high affinity of aptamer and target can lead to the alteration of the structure conformation of aptamer upon target binding.²⁴ Therefore, when the addition of its target, the binding between aptamer and its target will disturb the interaction of aptamer and GO, leading to the release of PS from the GO surface and restore SOG of the PS for PDT applications. As a result, we realize the regulation of SOG by binding with the target molecule.

2. Experimental procedure

2.1. Materials

Graphite powder (99%) was purchased from Alfa Aesar. Adenosine 5'-triphosphate (ATP, $\geq 99\%$), uridine 5'-triphosphate (UTP, $\geq 96\%$), cytidine 5'-triphosphate (CTP, $\geq 95\%$), guanosine 5'-triphosphate (GTP, $\geq 90\%$) were supplied by Sigma-Aldrich. Singlet oxygen sensor green (SOSG) and Hoechst were obtained from Life Technologies Co. Reactive oxygen species assay Kit was provided from the Beyotime Institute of Biotechnology (Shanghai, China). Other reagents were obtained from Beijing Chemical Reagent Co. All the chemicals used in this work were of analytical grade and were used as received without further purification. Fresh deionized water was used throughout the experiments.

Chlorin e6 (Ce6)-labeled ATP aptamer (AP-Ce6), complementary DNA (cDNA) and

random DNA (rDNA) were purchased from Takara Biotechnology Co. Ltd. (Dalian, China). The nucleic acids were high performance liquid chromatography (HPLC)-purified and freeze-dried. Stock solutions of DNA (10 μM) were prepared with Tris-HCl buffer (10 mM, containing 150 mM NaCl and 10 mM KCl, pH 7.40).

2.2 Preparation of Graphene Oxide

Graphite Oxide was synthesized using a modified Hummer's method according to the previous reports.^{17,25} Then, the as-prepared graphite oxide dispersion (~ 2.0 mg/ml) was sonicated by an ultrasonic probe (650 W, 35%) for 4 h in the presence of an ice bath to obtain a stable GO dispersion. After sonication, the dispersion solution was centrifuged to exclude any graphite oxide residue and large GO sheets.

2.3 Characterization

Fluorescence measurements were recorded using a Horiba JobinYvon FluoroLog3 spectrometer (Japan). Topping-atomic force microscopy (AFM) images of GO were taken on a scanning probe microscopy (SPM, Multimode 8, Bruke, USA) under ambient conditions. The fluorescence microscopy images were obtained using an inverted fluorescence microscopy (Olympus IX71). To measure the extent of co-localization between the fluorescence signals of Ce6 and dichlorodihydrofluorescein (DCF), an Image *J* plugin allowed for the calculation of the Pearson's correlation (R_r) and overlap coefficient (R). An overlap coefficient of higher than 0.6 indicates colocalization.

2.4 Test of Fluorescence Quenching Ability of Graphene Oxide

In a typical measurement, stock solution of AP-Ce6 was diluted 100-fold with Tris-HCl buffer (final concentration of AP-Ce6 is 100 nM), and then mixed with a certain concentration of GO. After the mixture was incubated at 37 $^{\circ}\text{C}$ for 1 h, the fluorescence was recorded from 600 nm to 700 nm with an excitation at 404 nm. As shown in Figure S2, the fluorescence intensity of AP-Ce6 decreased sharply as the concentration of GO increased from 1 $\mu\text{g}/\text{ml}$ to 4 $\mu\text{g}/\text{ml}$. When GO concentration was up to 5 $\mu\text{g}/\text{ml}$, the fluorescence intensity of AP-Ce6 was quenched down to *ca.* 1.14% of original fluorescence signal. As a result, 5 $\mu\text{g}/\text{ml}$ was taken as the optimized concentration for GO. In these conditions, the loading ratio of AP-Ce6 on GO is *ca.* 23.1%.

2.5 Validation of Fluorescence Response and Singlet Oxygen Generation of

Nanocomplex towards ATP in Solution

AP-Ce6 and GO were mixed in Tris-HCl buffer, and then the mixtures were incubated at 37 °C for 1 h to obtain the nanocomplex (GO/AP-Ce6). Thereafter, different concentrations of ATP were added to the above solution and the resulting mixtures were incubated at 37 °C for another 1 h. Finally, the fluorescence was measured with an excitation wavelength of 404 nm.

To evaluate SOG of GO/AP-Ce6 in solution, SOSG was used as an indicator for $^1\text{O}_2$ by fluorescence enhancement. In a typical procedure, after incubation at 37 °C for 1 h, the mixture was centrifuged to remove GO which might have some effects on detection of SOG. Then, SOSG was introduced into the above solution of GO/AP-Ce6 at the concentration of 2.0 μM . The mixture was placed in a cuvette and was irradiated at 404 nm, which was the maximum absorption of Ce6, for 10 min. Finally, fluorescence of SOSG was read out by measuring the fluorescence increase at 527 nm.

2.6 Selectivity

In order to investigate the fluorescence restoration and SOG of GO/AP-Ce6 which were caused only by ATP, 0.1 mM of ATP, GTP, CTP and UTP were mixed with GO/AP-Ce6, respectively. Thereafter, the mixtures were incubated at 37 °C for 1 h, and then the fluorescence of Ce6 was measured using the method as mentioned above. To test the SOG ability of GO/AP-Ce6 after incubated with ATP analogues, SOSG was added in the pre-treated solutions, and then the mixtures were transferred into the cuvettes and irradiated at 404 nm for 10 min. The SOSG fluorescence was read out spectrophotometrically using the similar protocol suggested above.

2.7 Cell Culture and Incubation Conditions

HepG2 (Human hepatocellular liver carcinoma cell line) cells were purchased from Wuhan Boster Biological Technology Ltd. (Wuhan, China) The cells were cultured in Iscove's Modified Dubecco's Medium (IMDM) supplemented with 20% fetal bovine serum (FBS, Gibco, Gland Island, NY, USA) in a humidified atmosphere of 5% CO_2 at 37 °C, and media was changed in every day. Untreated cells were kept in the dark or under light irradiation and taken as the reference standard. All the reported concentrations refer to the free AP-Ce6 equivalents.

2.8 *In Vitro* Cytotoxic Assay

To determine the cell viability under dark condition (*i.e.* without light treatment), the cells were seeded in 96-well plates at a density of 4000 cells/well and cultured in IMDM under a humidified atmosphere with 5% CO₂ at 37 °C for 24 h. Then seven groups of cell samples were set up as follows: group 1 with cells only (control); group 2 added GO to cells (labeled as GO); group 3 was incubated with ATP (labeled as ATP); group 4 added AP-Ce6 and GO (labeled as AP-Ce6+GO), group 5 was incubated with AP-Ce6 (labeled as AP-Ce6); group 6 was incubated with GO/AP-Ce6 (labeled as GO/AP-Ce6); and group 7 contained both GO/AP-Ce6 and ATP (labeled as GO/AP-Ce6+ATP). Each group had five parallel samples. After 24 h incubation at 37 °C with 5% CO₂, the cells were washed twice with phosphate buffered saline (PBS, pH 7.40), and then 200 µL of medium containing methyl thiazoyl tetrazolium tracer (MTT, 5 mg/ml) was added into each well. When the cells were further incubated for 4 h at 37 °C, the medium was removed, and replaced with 150 µL of dimethylsulfoxide (DMSO) to dissolve the MTT tetrazolium dye. After shaking for 10 min, the fluorescence of each well was then measured on a microplate reader (SpectraMax M2 MDC, USA) using 480 nm excitation and 530 nm emission wavelength. Throughout this process, the cells were kept in a dark environment without any light exposure.

To determine the cell viability when exposure to light, the cells were plated into each well at the density of 4000 cells/well. After being incubated for 6 h at 37 °C, the seven groups were treated with 650 nm light source at a power density of 50 mW/cm² for 20 min. After incubation for another 24 h, the standard MTT assay as mentioned above was carried out to determine the cell viability.

2.9 Validation of Fluorescence Response and Singlet Oxygen Generation of Nanocomplex towards ATP in Cancer Cells

A reactive oxygen species assay kit was applied to determine the level of intracellular ¹O₂. Briefly, the cells were seeded in the 96-well culture plates and allowed to attach for 24 h. Then, after the medium was discarded and washed three times with PBS, 100 µL of fresh medium containing dihydrodichlorofluoresceindiacetate (DCFH-DA) was added into each well and incubated at 37 °C for 20 min. Subsequently, the medium was discarded and washed with PBS again. Then, the cells were treated with the seven ways as mentioned above, and incubated for another 6 h at 37 °C. Next, the seven groups were irradiated with a 650 nm light

source at a power of 50 mW/cm². After irradiation for 20 min, the cells were washed twice with PBS and the fluorescence of DCF was measured on a microplate reader using 488 nm excitation and 525 nm emission wavelength. Cells treated with Rosup (a positive control reagent, 50 µg/ml) for 20 min were used as positive control.

All of the above experiments were repeated at least in triplicate and were statistically significant ($p < 0.05$).

3. Results and discussion

GO nanosheet was synthesized by sonication-assisted exfoliation of graphite oxide and possessed highly hydrophilic nature with a narrower size distribution (*ca.* 80 nm, Figure 2). AFM measurement reveals that the thickness of GO nanosheet is ~1.2 nm, indicating that a single-layer GO nanosheet was obtained.²⁶ Ce6 is used as the PS owing to its high photosensitizing efficacy.^{27,28} To test the feasibility of GO for regulation of SOG, ATP is used as a proof-of-concept target molecule. ATP is produced on the extracellular surface of cancer cells besides the mitochondrial matrix and relates to a large number of diseases.^{29,30} Therefore, the ATP specific linker is designed and then linked to Ce6.

The AP-Ce6 exhibits strong fluorescence emission in Tris-HCl buffer (pH 7.40) under the 404 nm excitation. However, as expected, its fluorescence gradually decreases with the addition of GO with different concentration (Figure S2). For example, up to 99% quenching of the fluorescence emission is observed when the concentration of GO increases to 5 µg/ml. However, after the addition of ATP (0.1 mM), the fluorescence is largely retained due to the formation of aptamer-ATP complex, which is increased by over 18 times as compared to that of AP-Ce6 in the presence of GO. These results imply that the interaction of AP-Ce6 and GO is much weaker than that of AP-Ce6 and ATP, thus causing AP-Ce6 to fall off the GO surface and ultimately resulting in the retention of its fluorescence (Figure 3a). That is to say, the ¹O₂ production ability of AP-Ce6 is largely restored after the addition of the target molecule. SOG was subsequently assayed by incubating the sample with SOSG and then irradiating at 404 nm for 10 min. SOG is evaluated in terms of the fluorescence intensity changes (F_1/F_0-1) of SOSG, where F_0 and F_1 are fluorescence intensities at 527 nm in the absence and presence of ATP, respectively, after subtracting the buffer background. In the case of GO/AP-Ce6 alone,

no noticeable fluorescence enhancement of SOSG is found (Figure 3a). While after the introduction of ATP (0.1 mM), the SOSG fluorescence of GO/AP-Ce6 exhibits a 25-fold enhancement. Furthermore, as the ATP concentration increased, the SOSG fluorescence is intensified, indicating more $^1\text{O}_2$ production after irradiation. When the concentration of ATP reaches up to 0.5 mM, no more fluorescence increase could be observed, reaching a plateau. It is worth noting that, when using free Ce6 instead of AP-Ce6, the quenching effect of SOG from GO/Ce6 complex appears to be less drastic compared to that of GO/AP-Ce6 complex, which is in agreement with the report by Liu et al.⁶ (Figure S3) Conclusively, these data support the hypothesis that both fluorescence and SOG of AP-Ce6 can be efficiently inhibited by GO. More significantly, they can be reversibly and quantitatively recovered on specific target treatments (Figure 3b and Figure S4).

It is known that aptamers have high binding affinity and specificity.^{31,32} To test this, GTP, CTP and UTP were used to evaluate the selectivity and target specificity of as-prepared GO/AP-Ce6. The results show that GO/AP-Ce6 exhibits much lower fluorescence enhancement response to the three analogues compared to that of ATP (Figure 4). This suggests that the $^1\text{O}_2$ production from GO/AP-Ce6 is indeed only triggered by ATP, without the detectable interference from other analogues.

We further evaluated the ability of GO/AP-Ce6 to generate $^1\text{O}_2$ in cells. Human HepG2 cells were first incubated with AP-Ce6 (0.4 μM) and GO/AP-Ce6+ATP (0.4 μM GO/AP-Ce6 and 40 μM ATP) for 6 h, respectively, and then irradiated with light (~ 650 nm) for 20 min. The intracellular $^1\text{O}_2$ levels in HepG2 cells were then measured using DCFH-DA method. The cells treated with Rosup were presented as the positive control. As shown in Figure 5, AP-Ce6 and GO/AP-Ce6+ATP triggered an increase in $^1\text{O}_2$ amount in cells by 245% and 411%, respectively. As control, HepG2 cells were also cultured with GO/AP-Ce6 and almost no increase of $^1\text{O}_2$ is observed in each sample. This is in good agreement with the previous investigation in the solution, further confirming SOG of GO/AP-Ce6 could be triggered by the addition of ATP. More evidence was obtained by fluorescence microscopy studies of HepG2 cells after the drug incubation (Figure 6 and Figure S5). Fluorescence images show a strong fluorescence of Ce6 in HepG2 cells incubated with AP-Ce6 and GO/AP-Ce6+ATP. However, HepG2 cells treated with or without GO/AP-Ce6 do not exhibit the Ce6

fluorescence. Furthermore, the high co-localization for DCF and Ce6 fluorescence further demonstrates that GO/AP-Ce6 is internalized near cell nuclei and then AP-Ce6 is cleaved by ATP, whereas almost no cleavages is found in the cells incubated with GO/AP-Ce6 (Table S1). These results indicate that GO/AP-Ce6 can enter cells, and its cleavage is specifically mediated by ATP at cell levels.

Next, we investigated the PDT efficacy of GO/AP-Ce6. The standard MTT assay was applied to determine the relative cell viability after 6 h post various treatments, normalized to the viability of cells not treated with drug or light (Figure 7). Without light exposure, nearly all of the cells are viable, exhibiting negligible dark toxicity (Figure 7a). Upon PDT treatment, GO/AP-Ce6 presents limited photodynamic cytotoxicity in HepG2 cells; however, GO/AP-Ce6+ATP significantly reduces the viability of the HepG2 cells (Figure 7b). These data indicate that GO/AP-Ce6 is specifically photoactivated by ATP, and its photodynamic cytotoxicity is ATP sequence-specific. Moreover, it is found that the cells treated with GO/AP-Ce6+ATP exhibits enhanced cytotoxicity compared to the HepG2 cells treated with AP-Ce6. This advance probably attributes to both the improved cellular uptake of Ce6 with the assistance of GO and the efficient protection of aptamers from enzymatic cleavage.³³ The fluorescence images clearly exhibits that GO/AP-Ce6+ATP treated cells show stronger Ce6 and DCF fluorescence compared to the cells treated with AP-Ce6, corresponding more uptake of Ce6 by cancer cells and more $^1\text{O}_2$ production. Similarly, the PDT efficiency of GO/AP-Ce6 against MDA, HeLa and ECV cells is better than that of AP-Ce6 alone (Figure S6).

4. Conclusion

In conclusion, we engineered a novel molecular nanocomplex of a PS, an aptamer and GO for controllable SOG. The fluorescence and photoactivity of the PS loaded on GO surface are quenched by GO in aqueous solution and cells, but are reversibly recovered after introducing a target molecule which could bind with aptamer to weaken the interaction between aptamer and GO, resulting in the release of the adsorbed PS from GO. Moreover, this nanocomplex shows enhanced uptake by the HepG2 cells compared to free PS, and in the absence of light it exhibits no major toxicity towards cells. In contrast, it induces significant cell death only in the presence of target molecules (*e.g.*, after reached target sites) with light irradiation. The

present findings firstly demonstrate that GO can function as a “cage” capable of controlling $^1\text{O}_2$ generation by the strong interaction between target molecules and AP-PS that is stronger than binding force between AP-PS and GO.

The present system displays several important advantages: (i) The design for selective regulation of SOG is versatile since different aptamer sequences can be designed for different target molecules (Figure S7,8). (ii) It is a hydrophilic system that possesses better biocompatibility than hydrophobic SOG systems. (iii) The use of GO as a nanocarrier to load drugs has been experimentally proved to be able to enhance drug loading efficiency and tumor uptake, and protect aptamers from enzymatic cleavage, which directly result in enhancement of the PDT efficiency and minimize its side-effects. (iv) GO/AP-Ce6 nanocomplex has a potential of integrating with contrast agents and theranostic drugs to form a theranostic agent that enables multimodal biomedical imaging with cancer therapy by PDT.

Supplementary Information

Electronic Supplementary Information (ESI) available: Details of other analysis.

Acknowledgment

This work was supported by National Basic Research Pro-grams of China (973 program, No. 2012CB932504), and National Natural Science Foundation of China (NO. 21320102003, 21001108 and 21177128).

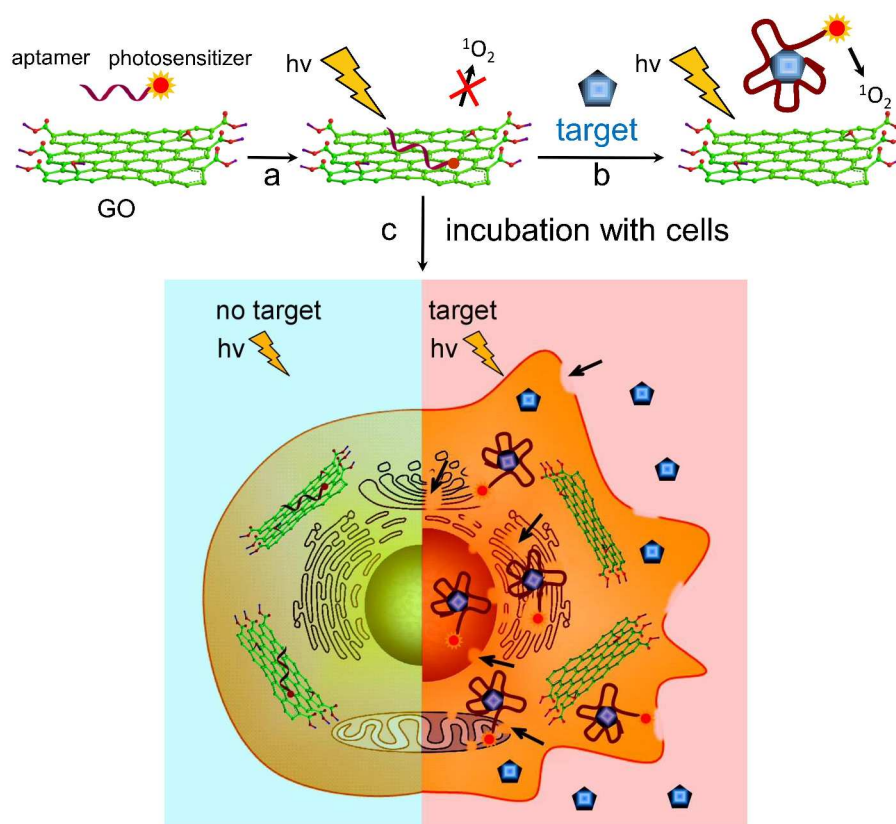


Figure 1. Schematic representation of nanocomplex and regulation of SOG upon target binding in solution and in cells: (a) AP-PS and GO were mixed together to form GO/AP-PS nanocomplex. (b) Restoration of SOG due to target binding. (c) Left: GO inhibits SOG without target molecules in cells; Right: GO restores SOG when target molecules present, finally killing cancer cells *in situ*.

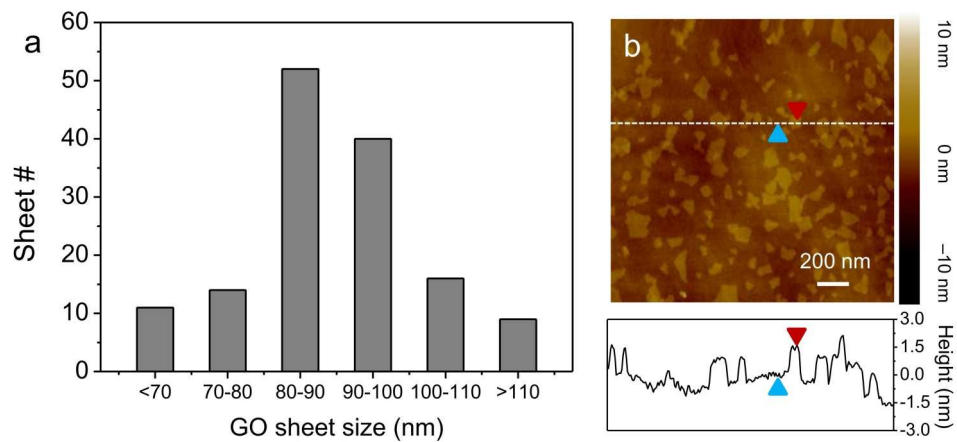


Figure 2. Characterization of GO nanosheets. (a) The lateral size histogram GO nanosheets observed by AFM. (b) AFM image and height profile of GO nanosheets. The line profile for nanosheets is marked by the white line in the image, indicating the thickness of the GO nanosheets.

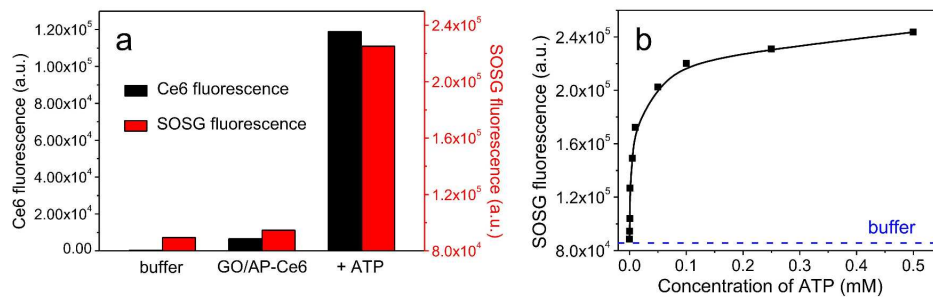


Figure 3. SOG regulation by aptamer-binding target. (a) The Ce6 and SOSG signals readout after 10 min of irradiation with excitation at 404 nm. (b) The SOSG signal plotted as the function of target molecule (ATP) concentration. The blue dotted line indicates the buffer's SOSG signal.

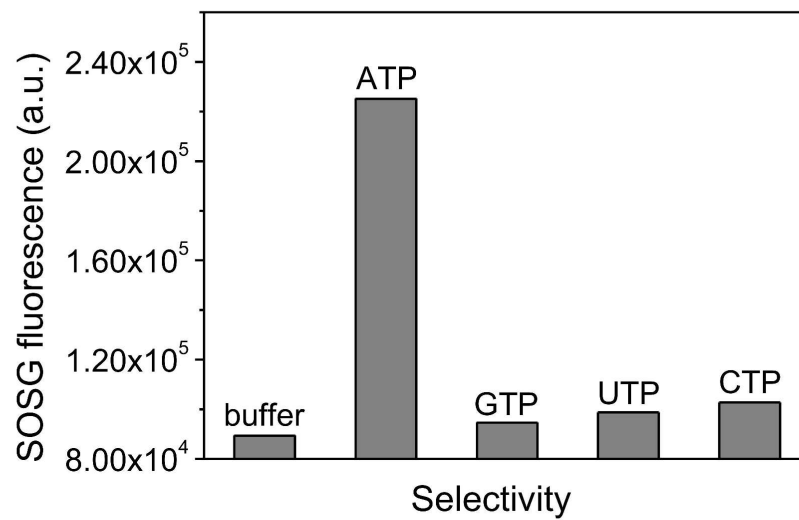


Figure 4. SOG specificity. The $^1\text{O}_2$ production of GO/AP-Ce6 shows high selectivity to ATP toward different ATP analogues: GTP, UTP, and CTP.

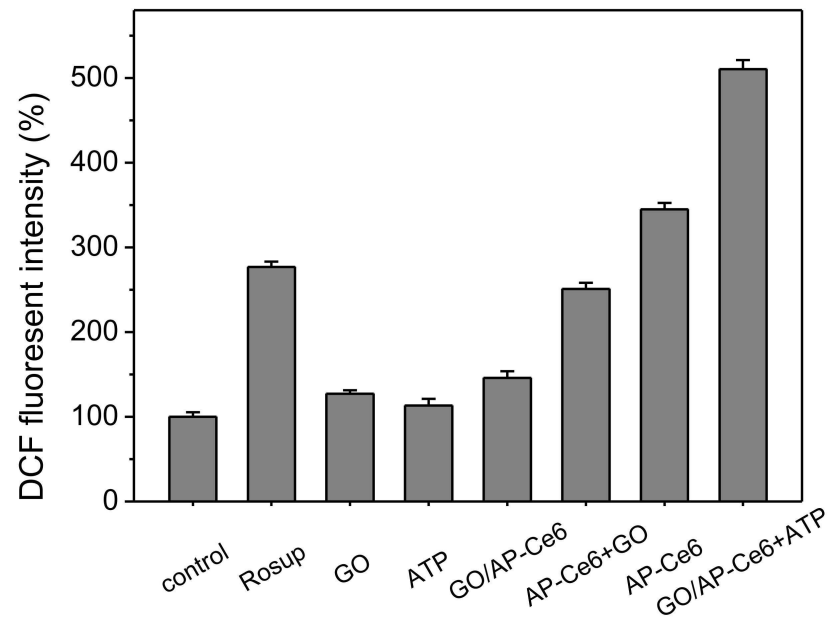


Figure 5. DCF-fluorescence intensity in HepG2 cells after treatment with nanocomplex.

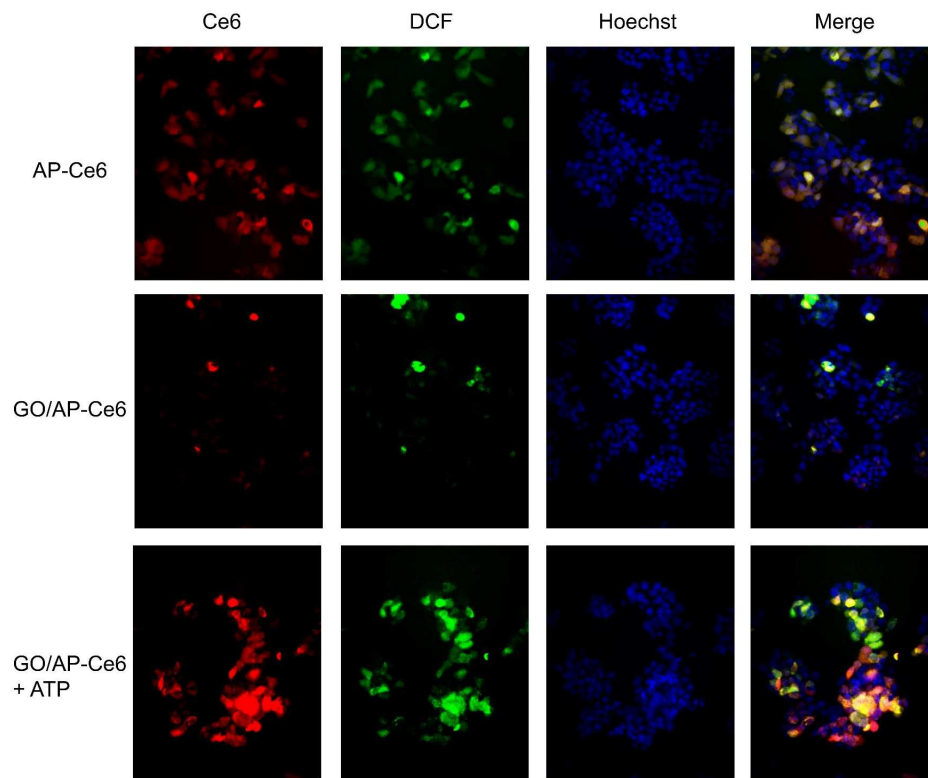


Figure 6. Fluorescence microscopy images of HepG2 cells incubated with AP-Ce6, GO/AP-Ce6 and GO/AP-Ce6+ATP.

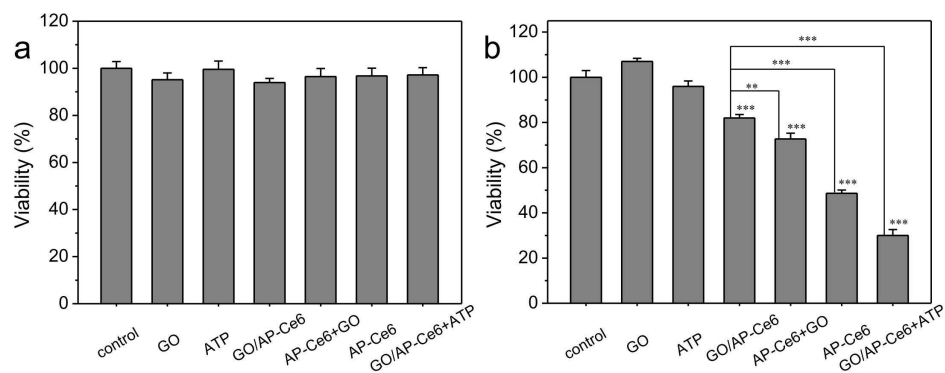


Figure 7. The cellular viability of HepG2 cells treated without (a) and with (b) light. (t test, * $p < 0.05$; ** $p < 0.01$; *** $p < 0.001$)

References

- 1 J. Chen, K. Stefflova, M. J. Niedre, B. C. Wilson, B. Chance, J. D. Glickson and G. Zheng, Protease-triggered photosensitizing beacon based on singlet oxygen quenching and activation, *J. Am. Chem. Soc.*, 2004, **126**, 11450-11451.
- 2 M. Colilla, B. González and M. Vallet-Regí, Mesoporous silica nanoparticles for the design of smart delivery nanodevices, *Biomater. Sci.*, 2013, **1**, 114-134.
- 3 D. K. Chatterjee, L. S. Fong and Y. Zhang, Nanoparticles in photodynamic therapy: An emerging paradigm, *Adv. Drug Deliv. Rev.*, 2008, **60**, 1627-1637.
- 4 N. M. Idris, M. K. Gnanasamandhan, J. Zhang, P. C. Ho, R. Mahendran and Y. Zhang, *In vivo* photodynamic therapy using upconversion nanoparticles as remote-controlled nanotransducers, *Nat. Med.*, 2012, **18**, 1580-1585.
- 5 D. E. J. G. J. Dolmans, D. Fukumura and R. K. Jain, Photodynamic therapy for cancer, *Nat. Rev. Cancer* 2003, **3**, 380-387.
- 6 B. Tian, C. Wang, S. Zhang, L. Feng and Z. Liu, Photothermally enhanced photodynamic therapy delivered by nano-graphene oxide, *ACS Nano*, 2011, **5**, 7000-7009.
- 7 K. Baba, H. E. Pudavar, I. Roy, T. Y. Ohulchanskyy, Y. Chen, R. K. Pandey and P. N. Prasad, New method for delivering a hydrophobic drug for photodynamic therapy using pure nanocrystal form of the drug, *Mol. Pharm.*, 2007, **4**, 289-297.
- 8 L. Zhou, W. Wang, J. Tang, J.-H. Zhou, H.-J. Jiang, and J. Shen, Graphene oxide noncovalent photosensitizer and its anticancer activity *in vitro*, *Chem.-Eur. J.*, 2011, **17**, 12084-12091.
- 9 T. Takemura, N. Ohta, S. Nakajima and I. Sakata, Critical importance of the triplet lifetime of photosensitizer in photodynamic therapy of tumor, *Photochem. Photobiol.*, 1989, **50**, 339-344.
- 10 H. Park and K. Na, Conjugation of the photosensitizer Chlorin e6 to pluronic F127 for enhanced cellular internalization for photodynamic therapy, *Biomaterials*, 2013, **34**, 6992-7000.
- 11 M. Ferrari, Cancer nanotechnology: opportunities and challenges. *Nat. Rev. Cancer*, 2005, **5**, 161-171.
- 12 Z. Zhu, Z. Tang, J. A. Phillips, R. Yang, H. Wang, and W. Tan, Regulation of singlet oxygen generation using single-walled carbon nanotubes, *J. Am. Chem. Soc.*, 2008, **130**, 10856-10857.
- 13 S. Y. Park, H. J. Baik, Y. T. Oh, K. T. Oh, Y. S. Youn and E. S. Lee, A smart polysaccharide/drug conjugate for photodynamic therapy, *Angew. Chem. Int. Ed.*, 2011, **50**, 1644-1647.
- 14 L. Yan, F. Zhao, S. Li, Z. Hu and Y. Zhao, Low-toxic and safe nanomaterials by surface-chemical design, carbon nanotubes, fullerenes, metallofullerenes, and graphenes, *Nanoscale*, 2011, **3**, 362-382.
- 15 L. Yan, Y. B. Zheng, F. Zhao, S. J. Li, X. F. Gao, B. Q. Xu, P. S. Weiss and Y. L. Zhao, Chemistry and physics of a single atomic layer: strategies and challenges for functionalization of graphene and graphene-based materials, *Chem. Soc. Rev.*, 2012, **41**, 97-114.

- 16 Z. Liu, J. T. Robinson, X. Sun and H. Dai, PEGylated nanographene oxide for delivery of water-insoluble cancer drugs, *J. Am. Chem. Soc.*, 2008, **130**, 10876-10877.
- 17 L. Yan, Y.-N. Chang, L. Zhao, Z. Gu, X. Liu, G. Tian, L. Zhou, W. Ren, S. Jin, W. Yin, H. Chang, G. Xing, X. Gao and Y. Zhao, The use of polyethylenimine-modified graphene oxide as a nanocarrier for transferring hydrophobic nanocrystals into water to produce water-dispersible hybrids for use in drug delivery, *Carbon*, 2013, **57**, 120-129.
- 18 K. Yang, L. Feng, X. Shi, and Z. Liu, Nano-graphene in biomedicine: Theranostic applications, *Chem. Soc. Rev.*, 2013, **42**, 530-547.
- 19 K. Yang, S. Zhang, G. Zhang, X. Sun, S.-T. Lee and Z. Liu, Graphene in mice: Ultrahigh *in vivo* tumor uptake and efficient photothermal therapy, *Nano Lett.*, 2010, **10**, 3318-3323.
- 20 P. Huang, C. Xu, J. Lin, C. Wang, X. Wang, C. Zhang, X. Zhou, S. Guo and D. Cui, Folic Acid-conjugated Graphene Oxide loaded with Photosensitizers for Targeting Photodynamic Therapy, *Theranostics*, 2011, **1**, 240-250.
- 21 L. Zhou, H. Jiang, S. Wei, X. Ge, J. Zhou and J. Shen, High-efficiency loading of hypocrellin B on graphene oxide for photodynamic therapy, *Carbon*, 2011, **50**, 5594-5604
- 22 F. Li, S.-J. Park, D. Ling, W. Park, J. Y. Han, K. Na and K. Char, *J. Mater. Chem. B*, 2013, **1**, 1678-1686.
- 23 E. Morales-Narváez and A. Merkoçi, Graphene oxide as an optical biosensing platform, *Adv. Mater.*, 2012, **24**, 3298-3308.
- 24 C. H. Lu, H. H. Yang, C. L. Zhu, X. Chen and G. N. Chen, A graphene platform for sensing biomolecules, *Angew. Chem. Int. Ed.*, 2009, **48**, 4785-4787.
- 25 W. S. Hummers and R. E. Offeman, Preparation of graphitic oxide, *J. Am. Chem. Soc.*, 1958, **80**, 1339-1339.
- 26 X. Li, G. Zhang, X. Bai, X. Sun, X. Wang, E. Wang and H. Dai, Highly conducting graphene sheets and Langmuir-Blodgett films, *Nat. Nanotechnol.*, 2008, **3**, 538-542.
- 27 J. D. Spikes and J. C. Bommer, Photosensitizing properties of mono-l-aspartyl chlorin e6 (NPe6): A candidate sensitizer for the photodynamic therapy of tumors, *J. Photochem. Photobiol. B: Biol.*, 1993, **17**, 135-143.
- 28 R. Rotomskis, J. Valanciunaite, A. Skripka, S. Steponkene, G. Spogis, S. Bagdonas and G. Streckyte, Complexes of functionalized quantum dots and chlorin e6 in photodynamic therapy, *Lith. J. Phys.*, 2013, **53**.
- 29 T.-C. Huang, H.-Y. Chang, C.-H. Hsu, W.-H. Kuo, K.-J. Chang and H.-F. Juan, Targeting therapy for breast carcinoma by ATP synthase inhibitor aurovertin B, *J. Proteome Res.*, 2008, **7**, 1433-1444.
- 30 Y. He, Z.-G. Wang, H.-W. Tang, D.-W. Pang, Low background signal platform for the detection of ATP: When a molecular aptamer beacon meets graphene oxide, *Biosensors Bioelectron.*, 2011, **29**, 76-81.
- 31 D. E. Huizenga and J. W. Szostak, A DNA aptamer that binds adenosine and ATP, *Biochemistry*, 1995, **34**, 656-665.
- 32 X. Liu, F. Wang, R. Aizen, O. Yehezkeli and I. Willner, Graphene

- oxide/nucleic-acid-stabilized silver nanoclusters: Functional hybrid materials for optical aptamer sensing and multiplexed analysis of pathogenic DNAs, *J. Am. Chem. Soc.*, 2013, **135**, 11832-11839.
- 33 Z. Tang, H. Wu, J. R. Cort, G. W. Buchko, Y. Zhang, Y. Shao, I. A. Aksay, J. Liu and Y. Lin, Constraint of DNA on functionalized graphene improves its biostability and specificity, *Small*, 2010, **6**, 1205-1209.

The table of contents

We engineered a novel nanocomplex of a photosensitizer, an aptamer and graphene oxide. The resulting nanocomplex could function as a “cage” for controlling singlet oxygen generation by manipulating the distance between graphene oxide and photosensitizers, and meanwhile use as the vehicle for more efficient delivery of photosensitizers to cancer cells, conclusively showing a controllable and enhanced photodynamic therapy.

